

# Topologically-based segmentation of brain structures from T1 MRI

SANAE MIRI<sup>1,2</sup>, NICOLAS PASSAT<sup>1</sup> and  
JEAN-PAUL ARMSPACH<sup>2</sup>

<sup>1</sup> LSIT, UMR 7005 CNRS/ULP, Strasbourg, France  
[passat@dpt-info.u-strasbg.fr](mailto:passat@dpt-info.u-strasbg.fr)

<sup>2</sup> LINC, UMR 7191 CNRS/ULP, Strasbourg, France  
[armspach@ipb.u-strasbg.fr](mailto:armspach@ipb.u-strasbg.fr)

## 1. Introduction

Cerebral structure segmentation from 3D MRI data is an important task for several medical applications. Brain segmentation methods can focus on specific structures such as the cortical surface [1], or intend to detect the principal parts of the brain [2]. Independently of their final purpose, they are primarily based on the classification of the intracranial volume into classes corresponding to the main cerebral tissues: cerebrospinal fluid (CSF), grey matter (GM), and white matter (WM). These classes present complex geometrical properties. However, they can be discriminated thanks to their distinct signal in modalities such as T1 or T2 MRI; moreover, the cerebral tissues present invariant and specific topological properties. Based on these assumptions, some topology-driven brain tissue classification techniques have been proposed [3, 4]. The method described in this short paper belongs to the same family of techniques, since its purpose is the classification of the brain into four classes: sulcal CSF, GM, WM, and ventricular CSF. As in [3], these classes are modelled (with some simplifying hypotheses) as hierarchically included spheres. Starting from a pre-segmentation based on this model, the four classes then evolve under photometric constraints. This process can be formalised as a discrete multi-class deformable model. From this point of view, it presents similarities with [5] (which however did not consider any topological constraints). It differs from [3], since the proposed method relies on a non-monotonic process, and from [4], since the classes *smoothly* evolve in a concurrent way.

## 2. Method

### 2.1 Input/output

The method takes as input a T1 MRI of the brain,  $I : E \rightarrow \mathbb{N}$  (with  $E = [0, d_x - 1] \times [0, d_y - 1] \times [0, d_z - 1]$ , generally  $[0, 255]^3$ ), from which the intracranial volume  $E' \subset E$  has been extracted, (Figure 1, 2<sup>nd</sup> picture), and two threshold values  $\mu_1 < \mu_2 \in \mathbb{N}$  de-

limiting the T1 signal intensity between CSF/GM, and GM/WM, respectively. The method output is a partition  $C = \{C_s, C_g, C_w, C_v\}$  of  $E'$ , where  $C_s$ ,  $C_g$ ,  $C_w$ , and  $C_v$  correspond to the sulcal CSF, GM, WM, and ventricular CSF classes, respectively.

### 2.2 Initialisation

The method starts from a presegmentation  $C^i$  of  $E'$  having the desired topology:  $C_v^i$  is simply connected (1 connected component, 0 hole, 0 cavity), and successively surrounded by  $C_w^i$ ,  $C_g^i$ , and  $C_s^i$  which are topological hollow spheres (1 connected component, 0 hole, 1 cavity), hierarchically organised, as illustrated in a 2D fashion in Figure 1 (1<sup>st</sup> picture). In  $\mathbb{Z}^3$ , such a model implies to choose dual adjacencies for the successive classes. The 6-adjacency has been considered for  $C_g^i$  (and thus  $C_v^i$ ), since GM is geometrically organised as a “thick” ribbon, while the 26-adjacency has been considered for  $C_w^i, C_s^i$ , since they both present thin details near the cortex. The initial presegmentation  $C^i$  is composed of a simply connected volume corresponding to  $C_v^i$ , surrounded by three “thick” closed surfaces, modelling  $C_w^i, C_g^i$  and  $C_s^i$ , their thickness corresponding to a coherent anatomical approximation (Figure 1, 3<sup>rd</sup> picture).

### 2.3 Deformable process

From a topological point of view,  $C^i$ , although composed of four distinct classes, can be considered as a binary image constituted of an object  $X = C_s^i \cup C_w^i$  and of the background  $\bar{X} = C_g^i \cup C_v^i$ , in a (26, 6)-adjacency framework. Based on this assumption, the segmentation process consists in modifying the frontier between  $X$  and  $\bar{X}$  in a topology-preserving fashion, under photometric constraints. This discrete deformable model process is algorithmically formalised at the end of the section. It firstly modifies the classification of the points which are, from a photometric point of view, the “most misclassified”. In order to preserve the topology of the initial model, only simple points [6] can be switched from a class to another. For simplicity’s sake, the algorithm is presented using set-based notations. However, it was implemented using efficient data structures (ordered FIFO lists), enabling to reach an optimal algorithmic complexity  $O(|E'|)$ , linear w.r.t. the size of the intracranial volume, since each point can be switched from one class to another only twice (the classification only depending on two threshold values).

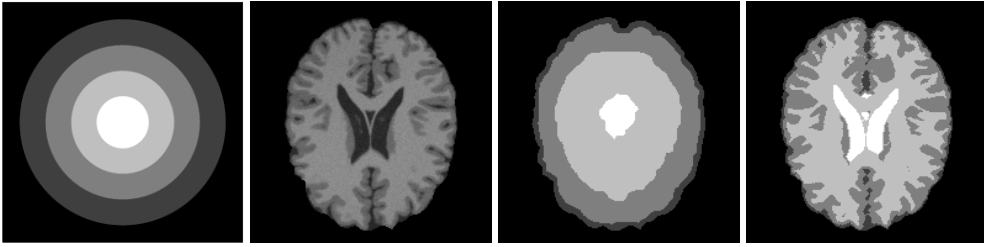


Figure 1. From left to right: topological model (from white to dark grey:  $C_v^i$ ,  $C_w^i$ ,  $C_g^i$ , and  $C_s^i$ ); T1 MRI ( $I_{|E|}$ : axial slice); initialisation of the segmentation process of the MRI ( $C_i$ ); result of the segmentation ( $C$ ).

---

```

repeat
1 - Frontier point determination
 $FP_{\{s,g\}} = (C_s^i \cap N_6^*(C_g^i)) \cup (C_g^i \cap N_{26}^*(C_s^i))$ 
 $FP_{\{g,w\}} = (C_g^i \cap N_{26}^*(C_w^i)) \cup (C_w^i \cap N_6^*(C_g^i))$ 
 $FP_{\{w,v\}} = (C_w^i \cap N_6^*(C_v^i)) \cup (C_v^i \cap N_{26}^*(C_w^i))$ 
/*  $N_k^*(A)$  is the set of points of  $\bar{A}$   $k$ -adjacent to  $A$  */
2 - Simple point determination
 $SP_{26} = \{x \in X \mid x \text{ is 26-simple for } X\}$ 
 $SP_6 = \{x \in \bar{X} \mid x \text{ is 6-simple for } \bar{X}\}$ 
3 - Candidate point determination
 $CP = (SP_6 \cup SP_{26}) \cap (FP_{\{s,g\}} \cup FP_{\{g,w\}} \cup FP_{\{w,v\}})$ 
/* Simple points at the frontier between two classes */
4 - Cost evaluation
for all  $x \in CP \cap FP_{\{s,g\}}$  (resp.  $FP_{\{g,w\}}, FP_{\{w,v\}}$ ) do
 $v(x) = I(x) - \mu_1$  (resp.  $I(x) - \mu_2, I(x) - \mu_1$ )
if  $x \in C_g^i$  (resp.  $C_w^i, C_v^i$ ) then
 $v(x) = -v(x)$ 
end if
end for
5 - Point selection and re-classification
if  $\max(v(CP)) > 0$  /* with  $\max(v(\emptyset)) = -\infty$  */ then
Let  $y \in CP$  such that  $v(y) = \max(v(CP))$ 
Let  $C_\alpha^i \in \{C_s^i, C_g^i, C_w^i, C_v^i\}$  such that  $y \in C_\alpha^i$ 
Let  $C_\beta^i \in \{C_s^i, C_g^i, C_w^i, C_v^i\}$  such that  $y \in FP_{\{\alpha,\beta\}}$ 
 $C_\alpha^i = C_\alpha^i \setminus \{y\}$ 
 $C_\beta^i = C_\beta^i \cup \{y\}$ 
end if
until  $\max(v(CP)) \leq 0$ 
 $C = C^i$ 

```

---

### 3. Experiments and results

Preliminary application of the method on the BrainWeb dataset seems to provide reasonably correct results. Quantitative validation works by comparison to the BrainWeb ground-truth are currently in progress. An example of segmented image is available in Figure 1 (4<sup>th</sup> picture). Depending on two parameters ( $\mu_1$  and  $\mu_2$ ), and relying on a linear complexity process, the proposed segmentation method enables to obtain results in a fast and easy way (computation time lower than 2 min. for a  $256^3$  image).

Nevertheless, this method only constitutes preliminary works, and is then not yet fully satisfying.

The deformation process is only guided by photometric constraints, neglecting high-level anatomical knowledge such as volumetric or thickness information. Moreover, the initial topological model does perfectly take into account structures such that the brainstem and the cerebellum, providing good results on the superior part of the brain (cortex region), but less correct ones on its inferior part.

A more sophisticated version of the method, involving a presegmentation topologically and anatomically closer from the reality, and using both photometric and geometric constraints to guide the deformable model process is under development and will be further submitted for publication.

### References

- [1] Y. Cointepas, I. Bloch, and L. Garnero, *Joined segmentation of cortical surface and brain volume in MRI using a homotopic deformable cellular model*, 3D Digital Imaging and Modeling - 3DIM'99, 2nd International Conference, Proceedings, Ottawa, Canada, 1999, pp. 240–248.
- [2] P. Dokládál, I. Bloch, M. Couprie, D. Ruijters, R. Urtasun, and L. Garnero, *Topologically controlled segmentation of 3D magnetic resonance images of the head by using morphological operators*, Pattern Recognition **36** (2003), no. 10, 2463–2478.
- [3] J.-F. Mangin, V. Frouin, I. Bloch, J. Régis, and V. López-Krahe, *From 3D magnetic resonance images to structural representations of the cortex topography using topology preserving deformations*, Journal of Mathematical Imaging and Vision **5** (1995), no. 4, 297–318.
- [4] P.-L. Bazin and D.L. Pham, *Topology-preserving tissue classification of magnetic resonance brain images*, IEEE Transactions on Medical Imaging **26** (2007), no. 4, 487–496.
- [5] M. Bosc, F. Heitz, and J.-P. Armspach, *Statistical atlas-based sub-voxel segmentation of 3D brain MRI*, International Conference on Image Processing - ICIP'03, 10th International Conference, Proceedings, Vol. 2, Barcelona, Spain, 2003, pp. 1077–1080.
- [6] G. Bertrand and G. Malandain, *A new characterization of three-dimensional simple points*, Pattern Recognition Letters **15** (1994), no. 2, 169–175.